Deep–Sea Research I 167 (2021) 103423

Contents lists available at ScienceDirect

Deep-Sea Research Part I

journal homepage: http://www.elsevier.com/locate/dsri

Synaphobranchid eel swarms on abyssal seamounts: Largest aggregation of fishes ever observed at abyssal depths

Astrid B. Leitner [a,b,*], Jennifer M. Durden [b,c], Craig R. Smith [b], Eric D. Klingberg [b], Jeffrey C. Drazen [b]

[a] Monterey Bay Aquarium Research Institute, 7700 Sandholdt Rd, Moss Landing, CA, 95039, USA
[b] University of Hawai'i at Manoa, 2500 Campus Rd, Honolulu, HI, 96822, USA
[c] National Oceanography Centre, European Way, Southampton, SO14 3ZH, UK

ARTICLE INFO

Keywords:
Baited camera
Deep sea
Abyss
Scavenger
Seamount
Clarion-clipperton zone
CCZ

ABSTRACT

The abyssal seafloor makes up three quarters of the ocean floor, and it is generally characterized as a food-limited habitat with low numbers of megafauna, particularly fishes. Baited camera observations from three abyssal seamount summits in the equatorial Pacific challenge this idea. On each of two deployments at the southernmost seamount, over 100 synaphobranchid eels (*Ilyophis arx*) were recorded feeding on standard bait (1 kg mackerel). This is the highest number of fishes per kg of bait ever recorded below 1000 m, including observations from large organic falls such as cetacean and shark carcasses. It is also the highest number that has ever been recorded at carrion of any kind or size at abyssal depths. We suggest an abyssal 'seamount effect' may be responsible, highlighting the potential importance of seamounts in structuring abyssal communities.

1. Introduction

About 75% of the seafloor is at abyssal depths (3000–6000 m), making it the largest benthic habitat globally (Harris et al., 2014; Priede, 2017). Though only a very small portion of this habitat has been sampled, explored, or even mapped, the existing body of abyssal work has generally characterized the abyssal ocean as food-limited, with low megafaunal abundances, especially for fishes, compared to shallower depths (Priede, 2017; Smith et al., 2008). Estimates of density and community composition for abyssal fishes in general vary globally, regionally, and locally due to environmental, oceanographic, and bathymetric conditions, as well as sampling methodology (Drazen et al., 2019; Fleury and Drazen, 2013; Leitner et al., 2017; Linley et al., 2017; Priede and Merrett, 1996; Yeh and Drazen, 2011). Mean densities are consistently low globally, ranging from 100s to a few 1000s of individuals per square kilometer across ocean basins as well as across topographic and oceanographic gradients (Bailey et al., 2006; Cousins et al., 2013; Drazen et al., 2019; Fleury and Drazen, 2013; Leitner et al., 2017; Linley et al., 2017; Merrett et al., 1991; Milligan et al., 2016; Pearcy et al., 1982; Priede and Merrett, 1996; Yeh and Drazen, 2011, also see Fig. 3c). Despite their low numbers, fishes play important roles in the abyssal ecosystem as scavengers and top predators (Drazen and Sutton, 2017). As predators, they exert top-down pressures that can control prey populations across wide scales, and as scavengers they redistribute organic carbon across the seafloor and influence energy flow and nutrient cycling in the deep sea (Drazen et al., 2008; Drazen and Sutton, 2017).

Abyssal fish communities are notoriously difficult to quantify. Trawls typically find lower abundances than visual transect methods (e.g. Cailliet et al., 1999; Lauth et al., 2004; Milligan et al., 2016), and some transecting studies are biased by some species' avoidance of noise and light (Ayma et al., 2016; Trenkel et al., 2004). Both due to this avoidance and low densities, visual transecting methods often report fishes in a very low percentages of frames; for example, one extensive camera survey (~71,000 images) on the northeast Atlantic abyssal plain reported fish in <0.3% of images (Milligan et al., 2016). Low observation rates make studying these important animals a challenge. Baited cameras provide an efficient and unobtrusive alternative method for observing large numbers of abyssal fishes, scavengers, and predators, as they mimic natural food falls where these animals naturally congregate and which make up a regular part of their diet (Drazen and Sutton, 2017; Priede, 2017). This method overcomes some of the challenges of low densities, high mobility, and high sensitivity by using bait to attract individuals from a surrounding area for census before a camera. Relative

* Corresponding author. Monterey Bay Aquarium Research Institute, 7700 Sandholdt Rd, Moss Landing, CA, 95039, USA.
E-mail address: aleitner@mbari.org (A.B. Leitner).

https://doi.org/10.1016/j.dsr.2020.103423
Received 19 September 2020; Received in revised form 22 October 2020; Accepted 23 October 2020
Available online 17 November 2020

abundances can be extracted from the image data and compared using a conservative relative abundance metric MaxN, the maximum number of individuals of a single taxon in a single video frame or photo. Since its inception (Priede et al., 1990), this measurement has become a standard relative abundance metric in the baited camera literature (e.g. Cappo et al., 2006; Drazen et al., 2019; Jamieson et al., 2017; Leitner et al., 2017; Linley et al., 2017; Priede and Merrett, 1996). In addition, absolute densities can be estimated given current speeds, fish swimming speeds, and times of first arrival (TOFA) or arrival rate by making some assumptions about fish distributions and behavior (Farnsworth et al., 2007; Priede et al., 1990; Priede and Merrett, 1996; Sainte-Marie and Hargrave, 1987). Mean densities calculated with these techniques can be comparable to other estimation methods (e.g. Priede and Merrett, 1996), although more recent studies have cast doubt on the utility of the TOFA method (Conn, 2011; Schobernd et al., 2014; Yeh and Drazen, 2009).

Here we report unprecedented observations of large aggregations of fishes (synaphobranchid eels) at baited cameras on abyssal seamounts in the western Clarion Clipperton Zone (CCZ) in the central Pacific Ocean, which challenge the paradigm of universally low abyssal fish density and show that abyssal seamount summits are capable of supporting high abundances of top predators and scavengers. We describe the estimated fish abundance, body mass, swimming speed and scavenger travel distances at an abyssal-depth seamount summit from baited camera video. We then compare the findings at this seamount to two further abyssal seamount summits in the western CCZ region. Finally, we review these findings in the broader context of global baited camera experiments and food falls to show that our observations represent the highest number of fishes ever observed at one time at abyssal depths, and the largest number of fishes ever observed per kg of carrion below 1000 m. We discuss these findings in the context of a 'seamount effect'.

2. Methods

2.1. Study area

All observations were made during the DEEPCCZ cruise aboard the RV *Kilo Moana* to the western CCZ in May–June 2018 (Drazen et al., 2019). This expedition investigated a single seamount and the adjacent abyssal plain in each of three Areas of Particular Environmental Interest (APEIs; Fig. 1 inset), areas protected from deep sea mining activities by the International Seabed Authority (Wedding et al., 2013). The seamounts were selected to have summits ≥1000 m above the abyssal plain and with flat areas suitable for lander deployments.

We focus primarily on observations from a previously unmapped, elongated abyssal seamount in the southeasternmost APEI (APEI 7; 4.9° N −141.7° W), with a summit depth of 3112 m (Fig. 1). For comparison, we also discuss observations from two additional abyssal seamount summits (3497 and 4218 m water depth) in APEIs to the northwest (APEI 4 and 1; 7.2° N −149.7° W and 11.5° N −153.7° W, respectively; Suppl. Fig. 1,2).

2.2. Environmental characterization

Seamount targets were chosen based on data from the Shuttle Radar Topography Mission (SRTM30 PLUS) 30 arc-second global bathymetry grid (Becker et al., 2009), which combines high resolution (~1 km) ship-based bathymetry data with ~9 km satellite-gravity data (http://topex.ucsd.edu/WWW_html/srtm30_plus.html). Upon arrival at the targeted seamounts, bathymetry data was collected using the R/V Kilo Moana's deep-water multibeam system (12 kHz Simrad EM120, Kongsberg Maritime, UK) while maintaining a ship speed of 8 knots. Raw pings were manually edited in near real time using the software Qimera. Sound velocity profiles were taken every 6 h during surveys. Processed multibeam bathymetry was then used to find suitable lander deployment sites (large, flat areas atop each seamount).

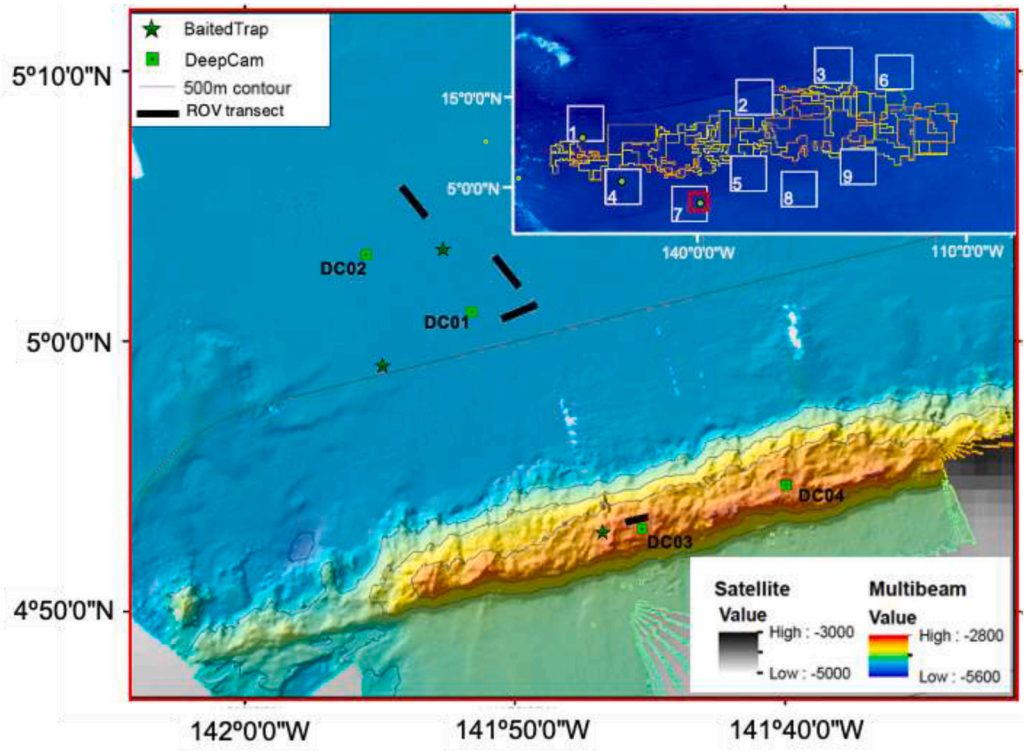

Fig. 1. Maps of the sampled area in APEI 7. Inset shows the focus seamount location (green point inside red rectangle) in the wider Clarion Clipperton Zone, with the Hawai'ian islands and the tip of Baja California for reference. Colored polygons are current mining exploration contract areas (orange) and mining reserved areas (yellow), and white numbered squares are Areas of Particular Environmental Interest. Other green points show the locations of the two additional seamounts sampled (locations in Table 2). The red rectangle shows extent of the detailed map showing the focal seamount; multibeam bathymetry (in color; depths in meters) overlays existing satellite estimated bathymetry (SRMT 30+ satellite bathymetry, greyscale). Green squares show locations of baited camera deployments. Green stars indicate baited trap locations. Black line segments represent ROV transects. Contour intervals are 500 m. The seamount base is at 4600 m depth, summit at ~3000 m, and seamount base widths (roughly north to south) at deployment locations are ~6.0 and ~7.0 km. (For interpretation of the references to color in this figure legend, the reader is referred to the Web version of this article.)

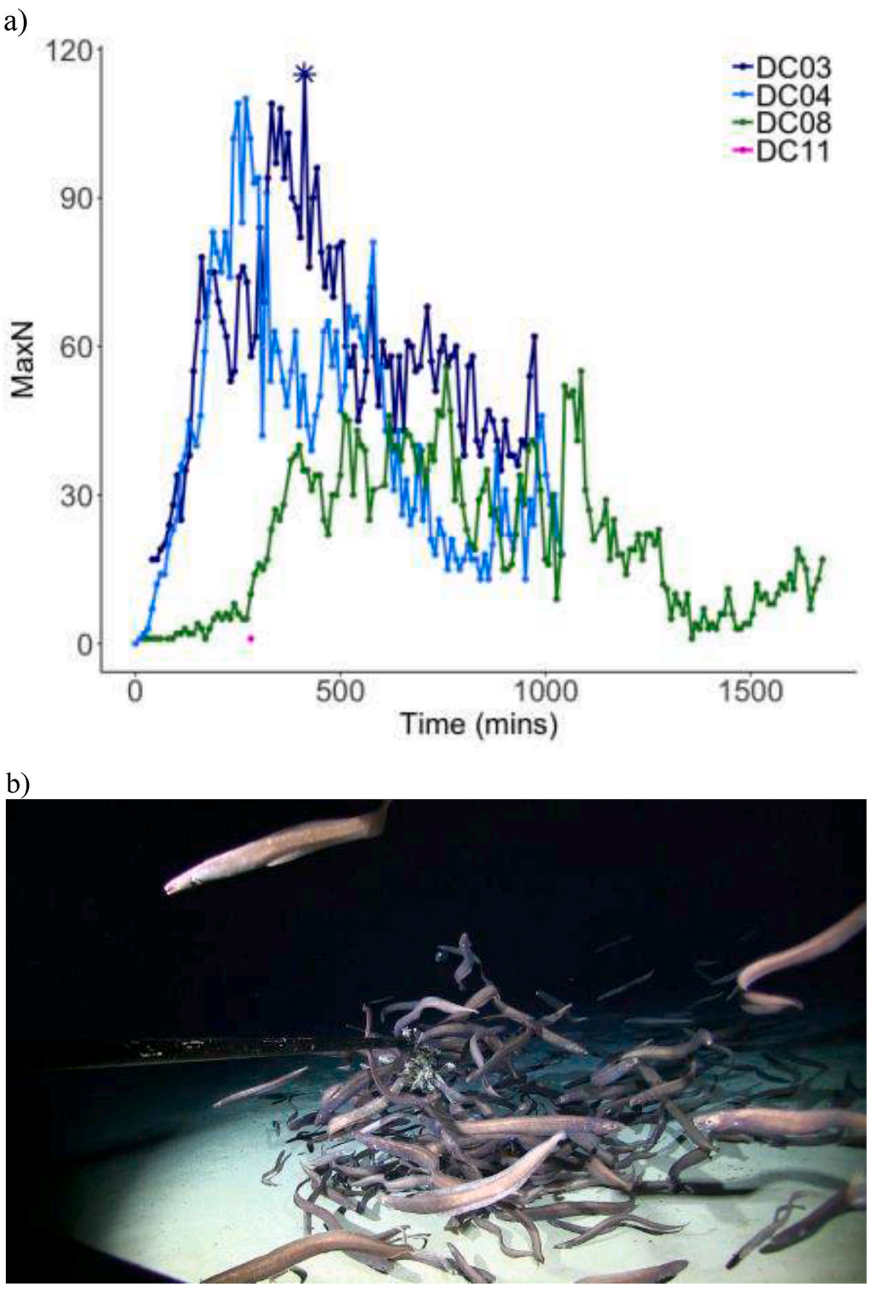

Fig. 2. a) MaxN (the single frame with the highest number of individuals of a single taxon) for each 2-min video clip for *Ilyophis arx* for each deployment versus time in min since lander touchdown on bottom. Blue lines represent deployments from APEI 7, the green line from APEI 4, and the magenta point represents the single observation of *I. arx* from APEI 1. DC12 is not shown on the plot because no eels were observed during that deployment. b) The synaphobranchid swarm at the bait from the first camera deployment on the abyssal seamount in APEI 7 at MaxN (N=115) for *Ilyophis arx*, which is the highest MaxN for all deployments and marked in a) by the star. This frame was captured 412 min after lander touchdown at a depth of 3083 m. (For interpretation of the references to color in this figure legend, the reader is referred to the Web version of this article.)

POC flux for each study location was estimated from data presented in Lutz et al. (2007). Decadal mean chlorophyll for each deployment site was calculated from monthly average 4-km resolution science quality satellite chlorophyll data obtained from the NASA Aqua MODIS satellite for the 10 years prior to the deployment date (https://coastwatch.pfeg.noaa.gov/erddap/griddap/erdMH1chlamday.html)). An upward-looking current meter (Aquadopp 6000, Nortek AS, Norway; 1.45 m above the seafloor) mounted on the baited camera system (see below) provided touchdown time, bottom depth and temperature, and current velocity measured at 1-min intervals.

2.3. Observations of bait-attending fish

2.3.1. Observations from baited video camera deployments

We used the DeepCam baited stereo camera video system (Leitner et al., 2017). This system is geometrically calibrated using the CAL software by SeaGIS (www.seagis.com.au) to provide precise measurement of both the field of view (1.86 m^2 seafloor calculated with direct measurements of field of view extent with the EventMeasure software by SeaGIS) and the animals in view. Deployment details appear in Table 1. Each deployment used 1 kg of mackerel (*Scomber* sp.) bait placed ~1.5 m in front of the camera lens.

Video was recorded for 2 min of every 10 min, with each recording period separated by an 8-min lights-off interval. The interval was chosen to maximize battery life while minimizing possible light disturbance on bait-attending animal behavior (e.g. Leitner et al., 2017). Total deployment bottom times ranged from 16.5 to 27.9 h.

All bait-attending and incidental megafaunal specimens observed in the video were enumerated and classified to the lowest possible taxonomic resolution, although for the purposes of this manuscript, we focus only on the synaphobranchid (cutthroat) eels (Johnson 1862; Teleostei infraclass and Anguilliformes order). Results from the entire bait-attending assemblage are to be reported in a subsequent paper (Leitner et al. in prep). Individual bait-attending synaphobranchid eels

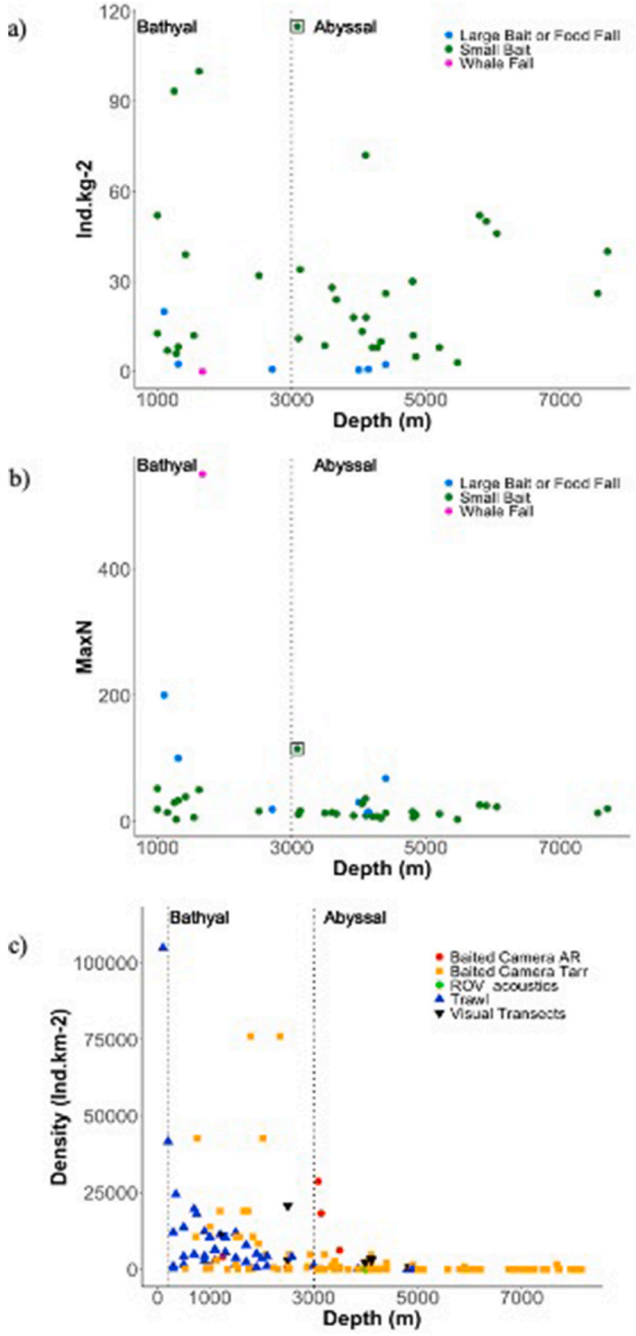

Fig. 3. A) Number (MaxN) of scavenging fish per kg of carrion by depth from reviewed papers and this study (denoted with black square) from all types of carrion: whale fall (magenta), large food falls and baited experiments (blue), and standard small (≤ 4 kg) bait experiments (green). All references are given in the supplementary data (see Suppl. Table 1). Only the maximum value is plotted from each study. Note that the number of fish per kg is less than 1 for the whale fall. Bathyal and abyssal depths are separated by the dotted line. B) Reviewed relative abundances (MaxN) across depths (from bathyal depths and deeper). Only the maximum value is plotted from each study. C) Estimated absolute fish densities in Ind.km^{-2} across depths from various methods: acoustics (green diamond), baited cameras with abundances estimated using the arrival rate method (red circles, Farnsworth et al., 2007) and using time of first arrival (orange squares, Priede and Merrett 1996), trawling (blue triangles), and visual transects (black downward triangles); see Suppl. Table 4 for data and sources. Estimated absolute abundances for this study calculated using the arrival rate method. (For interpretation of the references to color in this figure legend, the reader is referred to the Web version of this article.)

identified in the video were measured, where possible based on body position, using the stereo-video annotation software EventMeasure by SeaGIS. Due to the anguilliform swimming mode, measurement of eel total length was not possible. Instead, snout to pre-pectoral fin origin was measured. Measurements were only accepted if they met precision standards (i.e. Root Mean Square >10 mm, precision to length ratio <5%, precision <10 mm). These length measurements were used to derive estimated wet mass for each individual in the video using length-to-weight relationships from voucher specimens captured with baited traps.

2.3.2. Samples from baited trap deployments

Baited traps were deployed five times during the DeepCCZ cruise; twice on the abyssal plains in APEI 7, once on the seamount summit at APEI 7, once on the plain in APEI4, and one final deployment on the summit of the seamount in APEI 1 (Table 1). Specifications of the baited trap are provided in Leitner et al., (2017). Traps were deployed for a minimum of 22 h (22.7–47.1 h).

Eels were only captured in the trap deployed on the summit of the APEI 7 seamount. This trap was deployed in the same location as the first summit camera deployment (DC03) but on the following day (i.e. simultaneously with the DC04 camera deployment, 10.3 km away). Recovered specimens were enumerated and identified to the lowest taxonomic level possible. The snout-to-pectoral fin origin length and fresh wet weight were measured at sea (Suppl. Fig. 3a) using a spring scale, then specimens were fixed in 10% buffered formalin. Specimens were similarly measured and weighed again post-fixation on return to land. Exponential fits were calculated between length (snout to pectoral fin origin length) and (1) total body mass post-fixation in formalin and (2) estimated fresh body mass (Suppl. Fig 3b).

2.4. Bait-attendance statistics

2.4.1. Abundance estimations

Considerable debate exists about the best method for estimating true abundance from baited camera metrics (e.g. Farnsworth et al., 2007; Priede and Merrett, 1996; Schobernd et al., 2014; Stoner et al. 2008b). Early work in abyssal habitats used the time of first arrival (T_{arr}), average current velocity, and average swimming speed (Priede and Merrett, 1996):

$$n = 0.3849 \times \frac{\left(\frac{1}{f} + \frac{1}{w}\right)^2}{t^2} \qquad \text{>Equation 1}$$

Where f= fish swimming speed (m s^{-1}); w = mean current speed (m s^{-1}), t = time of first arrival (s), and where n = estimated density in fish per km^2.

Fish swimming speed was estimated by tracking the tip of the snout over time in three-dimensional space using the stereo-video software EventMeasure from SeaGIS. Each individual was tracked for as many frames as possible during a straight approach or departure, with a minimum of three point measurements per individual (1080i at 30 frames s^{-1}). Average speeds for each individual were used to calculate average speed for the taxon (arithmetic mean of mean individual speeds).

An alternative method based on arrival rate for the period between lander touchdown and the time of MaxN has also been used to estimate absolute densities from baited-camera data (Farnsworth et al., 2007):

$$n = \frac{AR \times (w + f) \times \sqrt{\pi^* \mu}}{(4 \times w \times f \times s)} \qquad \text{>Equation 2}$$

Where AR = the slope of the univariate non-linear regression of the number of fish with time over the time interval between lander touchdown and the time of MaxN, w = the mean current speed (m s^{-1}), f = fish net speed against current (approach speed), s = fish searching speed

Table 1
Summary of deployment details of the baited video camera system (DeepCam), baited trap and video surveys with a remotely-operated vehicle (ROV). Location, depth and dates for ROV surveys are start locations. Seabed area covered is calculated for each dive is the sum of each of the areas of each video transect calculated from each transect's total length and average width.

Equipment type	Deployment ID	APEI	Habitat	Latitude	Longitude	Water Depth	Deployment Date	Bottom Time	Seabed area covered
						(m)	(dd/mm/yy)	(h)	(m^2)
DeepCam	DC03	7	Seamount	4.8844	−141.755	3083	25/5/18	16.4	1.86
	DC04	7	Seamount	4.9114	−141.666	3140	26/5/18	17.4	1.86
	DC08	4	Seamount	7.2497	−149.6772	3497	5/6/18	27.9	1.86
	DC11	1	Seamount	11.5017	−153.6543	4218	11/6/18	17.5	1.86
	DC12	1	Seamount	11.5076	−153.5068	4346	13/6/18	12.7	1.86
Baited Trap	TR01	7	Plain	4.9854	−141.9151	4871	21/5/18	30.7	NA
	TR02	7	Plain	5.0571	−141.8778	4871	23/5/18	47.1	NA
	TR03	7	Seamount	4.8826	−141.7793	3203	26/5/18	25.1	NA
	TR04	4	Plain	7.2156	−149.8283	4872	4/6/18	43.3	NA
	TR05	1	Seamount	11.5015	−153.6175	4175	11/6/18	22.7	NA
ROV survey	LK-086	7	Plain	5.1151	−141.8965	4862	25/5/18	2.75	4304
	LK-088	7	Seamount	4.8879	−141.7572	4877	27/5/18	2.5	2995
	LK-089	7	Plain	5.0602	−141.8311	3137	28/5/18	4.5	8048
	LK-090	4	Plain	7.0363	−149.9395	3567	1/6/18	1.7	3714
	LK-091	4	Plain	6.9876	−149.9123	5050	2/6/18	3	8637
	LK-092	4	Seamount	7.2648	−149.774	5007	3/6/18	3.5	2951
	LK-094	4	Plain	6.9875	−149.9327	5001	6/6/18	3	8377
	LK-095	1	Plain	11.2751	−153.7445	5247	9/6/18	4	9557
	LK-096	1	Plain	11.2526	−153.6061	5216	10/6/18	2.3	8649

Table 2
Environmental data (including measured parameters and particulate organic matter flux estimated from Lutz et al., 2007, and decadal mean chlorophyll-a from MODIS Aqua) for baited camera locations and estimated MaxN values.

Deployment ID	Location		Lat	Long	Depth	POC flux	Decadal Avg Chl	Temp	Avg Speed	Max Speed	MaxN	Time of MaxN	Time of first arrival
	APEI	Habitat			(m)	(mgC m^{-2} d^{-1})	(mg m^{-3})	°C	m s^{-1}	m s^{-1}	*Ilyophis arx*	(min)	(min)
DC01	7	Plain	5.018	−141.860	4878	1.85	0.147	1.62	0.05	0.12	0	NA	NA
DC02	7	Plain	5.053	−141.926	4860	1.85	0.147	1.62	0.05	0.12	0	NA	NA
DC03	7	Seamount	4.884	−141.755	3083	1.97	0.147	1.8	0.06	0.14	115	412	NA
DC04	7	Seamount	4.911	−141.666	3140	2.01	0.147	1.79	0.08	0.18	110	269	11.3
DC05	4	Plain	7.052	−150.011	5216	1.38	0.117	1.67	0.09	0.13	0	NA	NA
DC06	4	Plain	7.029	−149.902	5004	1.43	0.117	1.64	0.08	0.14	0	NA	NA
DC07	4	Seamount	7.270	−149.783	3542	1.33	0.116	1.68	0.05	0.15	NA	NA	NA
DC08	4	Seamount	7.250	−149.677	3497	1.43	0.116	1.7	0.04	0.16	56	758	20.2
DC09	1	Plain	11.249	−153.761	5236	1.10	0.073	NA	NA	NA	0	NA	NA
DC10	1	Plain	11.252	−153.643	5213	1.16	0.073	NA	NA	NA	0	NA	NA
DC11	1	Seamount	11.502	−153.654	4218	1.16	0.071	NA	NA	NA	1	282	281.7
DC12	1	Seamount	11.508	−153.507	4346	1.12	0.072	NA	NA	NA	0	NA	NA

(assumed here to be equal to approach speed), $\mu = 10^{-3}$, a constant representing the rate of reorientations.

The regression model to be used for estimating AR following the recommendations of Farnsworth et al. (2007) is:

$$N_t = AR \times t^{3/2} \quad \text{>Equation 3}$$

Where N_t = number of fish (N) after applying the transformation $N_t = \sqrt{N} + \sqrt{N+1}$, so that the distribution of N_t is approximately normal.

Where possible, we used both methods for comparison to published values. However, there are several issues in applying the T_{arr} method to this dataset. The first 40 min of our first deployment were not recorded, and there is considerable uncertainty in the time of first arrival in the second deployment (±8 min) due to the fast arrival of the animals of interest and the imaging interval used. The T_{arr} method is highly sensitive to small changes in time of arrival, especially with rapid first arrival times (less than ~20 min), and model results have been highly variable and not always significantly correlated to true abundances (Farnsworth et al., 2007; Schobernd et al., 2014; Stoner et al. 2008a; Yeh and Drazen, 2011).

A third approach to measuring relative abundance for standardized baited camera deployments is the use of MaxN. MaxN is the most widely reported metric in baited camera literature and is a conservative metric generally well correlated to absolute abundances (e.g. Stoner et al., 2008). This metric was extracted for each 2-min video clip over the course of one deployment and for each entire deployment. This metric was used as a relative abundance metric following standard practices throughout the literature (Cappo et al., 2006a; Misa et al., 2016; Sackett et al., 2017; Schobernd et al., 2014; Stoner et al. 2008a).

We focus the present analysis on the use of MaxN and the arrival rate (AR) method for estimating absolute abundance, though results from the time of first arrival method (T_{arr}) are also reported.

2.5.1. Distance estimations

Maximum possible scavenger travel distances, *d*, to the bait were estimated following the methods of Priede and Merrett (1996). The distance from which a scavenger has traveled to arrive at the bait was calculated using the deployment length (t_T) in place of t_{arr}, because the deployment length gives the last possible time a scavenger could have arrived at the bait and still be captured on video. In addition, the calculation uses the average current speed, which determines the time it takes the bait plume to travel through the water and reach a fish

(assuming that fish is motionless before bait plume detection), and the average swimming speed of the fish, which estimates the speed at which the fish can travel toward the bait (assuming a fish travels to the bait no faster than its average swimming speed).

Following the assumptions of fish behavior and distributions made by Priede and Merrett (1996) and the equations given therein, the furthest distance from which a fish could have been attracted to the bait (d) is given by:

$$d = \frac{t_T{}^{*}w{}^{*}f}{(w+f)} \quad \text{>Equation 4}$$

Where t_T is the total deployment time, w is the average current speed that spreads the bait plume, and f is the average fish swimming speed. This does not take into account attraction to the bait following other stimuli like sound or motion generated by animals already feeding at the bait, which can also attract scavengers (Auster et al., 2020). From this, distance and maximum attraction area can also be calculated (Priede and Merrett 1996). A theoretical upper limit to distance traveled by any observed fish (d_{max}) is also a useful statistic. If a fish swam directly at the bait in a straight line by chance (not as a result of bait plume detection), a fish could only arrive from as far away as d_{max}, which is simply the product of the fish's swimming speed and the total deployment time.

2.6. ROV video surveys

Observations of fishes in seabed video transects were used to provide additional context to the data from the baited video. Video footage was captured using a video camera (Mini Zeus MK I, Insite Pacific, USA) mounted at an oblique angle to the front of the ROV *Lu'ukai* (Fig. 1). Seabed transects were conducted with the vehicle moving at 0.5 Kn, at a target camera altitude of 1.78 m), with the target length of each transect being ~1000 m. Parallel lasers with a spacing of 0.148 m were used for scaling. Fishes observed during video transects were enumerated and identified to the lowest taxonomic level possible. ROV transects were available for comparison in both seamount and plain habitats for APEI 7 and 4; however, only abyssal plain transects were conducted in APEI 1.

2.7. Literature review

To provide broader context to our baited video observations, we undertook a comprehensive literature review of abyssal baited camera and food fall experiments, as well as observations at natural food falls and carcasses. This yielded 33 papers for review. Given the relative paucity of data, we also included similar observations deeper than 1000 m water depth. In total, 47 relevant papers were included (Suppl. Table 1). We extracted the water depth, location, and type of experiment or observation as well as the highest MaxN of fishes recorded in the paper, the taxa of this record MaxN, the viewable area or surveyed area, and the amount and type of bait or carrion used in the study. These data allowed us to compare our findings to literature-derived estimates of relative abundances (MaxN) and the maximum number of fish observed at one time per kg of carrion.

3. Results

3.1. Environmental setting

Decadal average surface primary productivity for study area in APEI 7 is 0.147 mg m^{-3}. Estimated seafloor particulate organic carbon (POC) flux at the abyssal seafloor in this region is 1.99 mg C_{org} m^{-2} d^{-1} (Lutz et al., 2007), and measured fluxes at 700 m above bottom near to the site are about 310 μmol C_{org} m^{-2} d^{-1} (Smith et al., 1997). APEIs 4 and 1 had lower average surface primary productivity and estimated seafloor POC fluxes (1.4 and 1.2 mg C_{org} m^{-2} d^{-1}) than APEI 7, suggesting a gradient of declining productivity and food availability to the northwest.

The substrate at the APEI 7 seamount deployment locations (3083 and 3140 m water depth) was bright white, furrowed sand with no manganese nodules or hard substrate of any kind. It is worth noting that the surrounding abyssal plain also had no nodules. Both deployments were within large, circular flat areas (diameter ~1500 m) on the seamount (see Table 1 for metadata summary) and surrounded by rough, hard substrate and complex topography. Bottom temperatures ranged from 1.7 to 1.8 °C, and arithmetic mean current speeds 1.45 m above the seafloor ranged from 0.04 to 0.08 m s^{-1}. Maximum recorded current speeds were 0.142 and 0.175 m s^{-1}, respectively. This APEI is under the influence of equatorial upwelling (National Oceanic & Atmospheric Administration, Smith and Demopoulos, 2003). The adjacent abyssal plain is at approximately 4869 m water depth, where the seabed was composed of soft, muddy sediment.

Deployments on the seamounts in APEI 4 and 1 likewise had similar white, sandy substrates with no manganese nodules and were within similar flat areas on the summits. Due to loss of the current meter upon the ninth recovery, temperatures and current speeds are not available from APEI 1. The deployments on the APEI 4 seamount recorded the same temperature range and current range as on the APEI 7 seamount, though average current speed was lower (~0.05 m s^{-1}). It should be noted that across all deployments there was no significant difference between average current speeds recorded in seamount versus in plain habitats, but maximum recorded current speeds were significantly higher on seamounts (Table 2). Both summit depths and abyssal plain depths increased to the northwest. The approximate seamount summit depth in APEI 4 was 3497 m and the plain depth 5109 m (Suppl. Fig. 1, Table 1). The summit depth in APEI 1 was 4218 m and the plain depth 5224 m (Suppl. Fig. 2, Table 2).

3.2. Observations of bait-attending fish

We observed swarms of >100 cutthroat eels (family Synaphobranchidae) at the bait in video captured on the seamount in the southeasternmost APEI (7), 56 at the seamount in the midlatitude APEI (4), and a single individual at the seamount in the northwesternmost APEI (1).

3.2.1. Specimen identification and sizing

From the baited video, the eels were identified to the genus *Ilyophis*. The 12 voucher specimens trapped on APEI7 seamount were identified as *Ilyophis arx*. Mean total length of the trapped specimens was 0.398 m (range 0.231–0.551 m). Mean wet mass was 113.2 g (23.5–300 g), and a mean post-fixation mass was 86.6 g (9–244 g) (Suppl. Table 2). For both mean wet mass and mean post-fixation mass, the best mass-length relationships were exponential fits with snout to pectoral fin origin length (PPFL; Suppl. Fig. 3, $r^2 = 0.91$ for both).

Size distributions for the individuals recorded in the baited video were similar on both seamounts where eels were observed with a mean PPFL of 6.0 cm (SD 1.0 cm) in APEI and 6.1 (SD = 1.6 cm) at the APEI 4 seamount. Using the mass-to-PPFL relationship derived from trapped specimens, the mean estimated wet weight of eels on both seamounts was 66 g. Using the PPFL-to-total-length relationship from the trapped specimens, the mean total length of observed eels was estimated at approximately 0.37 m.

Mean swimming speed for *Ilyophis arx* was determined to be 0.074 ± 0.064 m s^{-1}.

3.2.2. Bait attendance

During the first seamount deployment (DC03), a MaxN of 115 eels was recorded at 412 min after the lander reached the bottom (Fig. 2, T_{arr} density estimate = NA, AR density estimation = 18266 individuals km^{-2}). During this deployment, the first 41 min on bottom were unfortunately not recorded, so T_{arr} density estimation was not possible; however, a maximum of 17 eels were visible in a single frame in the first available video. During the second deployment (DC04) on this same

seamount ~1000 m from the first (DC03), a MaxN of 110 individuals was recorded 269 min after lander arrival on bottom. In this deployment, the first eel was observed during the first video period, 11.3 min after the bait arrived on the bottom (T_{arr} density = 560 Ind.km^{-2}, AR density = 28687 Ind.km^{-2}). Due to the recording interval, touchdown was not captured on video so the true first arrival time could be as short as 3.3 min, giving an upper T_{arr} density estimate of 6593 Ind.km^{-2} (Suppl. Table 3 summarizes all abundance metrics for all deployments discussed). MaxN exceeded 100 in 4 video clips for each seamount deployment in APEI 7. In both deployments, eels arrived rapidly and quickly accumulated at the bait (Fig. 2a). MaxNs were recorded at a time when the majority of the bait was consumed, and generally, numbers gradually declined after this 'feeding frenzy' stage, although eels were present in 100% of videos after the first arrival during both deployments.

At the deployment on the seamount in APEI 4 (DC08, Suppl. Fig. 1 inset), the first eel was seen 20 min after touchdown, and numbers accumulated much more gradually to a MaxN of 56 at 758 min (Fig. 2a, Suppl. Fig. 1). At the deepest and northernmost seamount sampled, 1501 km away in APEI 1 (DC11, Suppl. Fig. 2), a single eel was seen at the bait during one video sequence, 282 min after lander touchdown, and a subsequent deployment (DC12) did not observe any eels (Fig. 2a).

Ilyophis arx was not the only species observed in these deployments. Several species of cusk eels (Ophidiidae), large shrimps (Penaeidae), and grenadiers (Macrouridae) were also observed, and patterns in community structure and diversity will be discussed elsewhere (Leitner et al. *in prep*).

There are several notable differences between the two deployments on the seamount in APEI 7 (Fig. 2a). While the increase in numbers of eels in the initial 125 min of both deployments is nearly identical, afterwards the pattern is shifted in time between the two deployments. MaxN was reached much faster in the second deployment (at 250 min versus at over 400 min), and there was a small second wave of animals around 600 min, giving the curve for this deployment a primary and a secondary peak. The deployment at the second seamount had a similar bimodal pattern, though accumulation was much slower, and peak numbers were nearly half those recorded at the first seamount. In DC03, no bimodal pattern was observed. In contrast, once MaxN was reached, albeit much later, the numbers decreased steadily as individuals left the field of view once the majority of the bait was consumed (likely satiated).

All available data suggest that these eels are exclusively found in the seamount habitat. An eel tracking the bait plume at the average measured swimming speed (0.074 m s^{-1}) and arriving in the last video clip could have arrived from a maximum distance of 2.0–2.3 km, based on the deployments in APEI 7. These distances are smaller than half the seamount width (Fig. 1). The theoretical maximum possible distance traveled by any observed eel to the camera (the product of the average swimming speed and the bottom time of the longest deployment) is less than 4.6 km. This theoretical maximum distance is also less than half the seamount width. Additionally, this species was not observed on any of the baited camera deployments conducted on the surrounding abyssal plain (Fig. 1 and Suppl. Fig. 1, 2). Therefore, it is likely that these eels are purely seamount-associated animals.

3.3. Observations in ROV-based video surveys

Eight eels were observed during the ROV transect conducted on the APEI 7 seamount (2995 m^2 surveyed, local density 2671 Ind.km^{-2}), and one individual was observed on the single available ROV transect conducted on the APEI 4 seamount (2951 m^2 surveyed). No eels were seen during any of the 3 ROV transects conducted on the surrounding abyssal plain in APEI 7 (12,352 m^2 surveyed total), or during any ROV transects on abyssal plains in APEI 1 or 4 (see Table 1 for transect details). All eels swam away from the ROV as they were approached.

3.4. Context from literature review

The comprehensive literature review found that the observations presented here are the highest recorded number of fishes ever seen at one time (in a single frame) at or below 3000 m worldwide. When considering only small bait packages (≤4 kg), these observations represent the highest numbers of fish scavengers ever recorded below 1000 m. Note that the bait used in these deployments (1 kg of mackerel, *Scombrus* sp.) is one of the most widely used, standard baits. Observations with much larger baits (10s–10000 s kg of carrion) were also reviewed. These have a much stronger bait plume and are likely a more attractive food source with a greater potential to attract high numbers of fishes. While the diffusion of a bait plume depends on the current regime, at abyssal depths average flow conditions are generally similar across sites, with average speeds around 0.05 m s^{-1} (e.g. Priede, 2017). Additionally, faster average current speeds have not been found to correlate with higher relative abundances at abyssal depths (Leitner et al., 2017; Linley et al., 2017). Across all abyssal studies of large food falls in our review, the average MaxN was 17 individuals (SD=13, range 3–68) (Fig. 3b). Therefore, even when including data from much larger bait parcels (up to 53 kg), our observations at the APEI 7 seamount remained the highest ever recorded at abyssal depths. In fact, these observations lie more than 7 standard deviations from the previous abyssal mean MaxN, and even the APEI 4 observations of 56 eels lies more than 3 standard deviations from the previous mean. We further found that this was the highest recorded number of carrion-attending fishes per kilogram of carrion ever observed below bathyal depths (≥1000 m). The results of our literature review are summarized in Suppl. Table 1 and in Fig. 3.

Observations of similar magnitudes were only recorded in studies at bathyal sites (at least 1000 m shallower) using carrion/bait at least four-fold larger than used in this study. For example, several hundred hagfish (family Myxinidae, *Eptatretus deani*) were reported at two large whale falls (thousands of kg of carrion each) off of southern California at 1670 m and around 100 hagfish at a 40 kg bait package in the same area (Smith, 1985; Smith et al., 2002). Additionally, over 200 hagfishes (*Myxine* cf *fernholmi*) were observed at the 20 kg carcass of a Patagonian toothfish (*Dissostichus eleginoides*) at 1100 m in the Falkland Islands (Collins et al., 1999). Interestingly, at bathyal depths (1000–3000 m), aggregations of the order of magnitude recorded in this study have only been previously reported for hagfishes. Even when including this bathyal data, our observations remain the highest number of fish (115 Ind.kg^{-1}) ever recorded per kg of carrion below 1000 m globally.

4. Discussion

Large swarms of eels of the species *Ilyophis arx* were observed at bait on three geomorphically similar abyssal seamounts but not on surrounding plains in the western CCZ with over 100 individuals observed at a single 1-kg bait package in some instances. The southernmost seamount had the highest recorded relative abundances (MaxN = 115), and abundances declined to the north. A literature review revealed that the southernmost observations are the highest recorded relative fish abundances in the abyssal ocean globally at bait/carrion of any size. We interpret these results as evidence of a localized eel hotspot attributable to a seamount effect. In addition, the relative abundance of eels observed at the midlatitude seamount was also higher than all but one of the studies reviewed here.

It must be noted that it can be difficult to compare different baited lander and food fall studies because bait type, field of view, deployment durations, imaging intervals, lander geometries (when explicitly reported) and flow regimes vary between studies (including the studies reviewed here). Each of these factors is known to influence the results of baited lander and food fall experiments, and this must be kept in mind when making comparisons between these studies (Fleury and Drazen, 2013; Yeh and Drazen, 2011). In our comparisons, the durations of the

observations are all similar and well in excess of times of MaxN for most species, and bait packages are generally small (0.5–2 kg) oily fish (scombrids). Additionally, Hardinge et al. (2013) showed that the amount of bait, when relatively small (ranging from 0.2 to 2 kg), had no significant impact on the relative abundance and numbers of species sampled in baited experiments. We also purposefully compared our small bait package deployments to large food fall experiments and observations (with a stronger bait plume likely to attract greater numbers of scavengers) to emphasize how unexpected our observations are in the larger context.

It is difficult to estimate true abundance from baited camera data, and MaxN is a relative abundance metric. However, MaxN is the most widely reported metric across the baited camera literature from the shallow water (e.g. Cappo et al., 2006; Schobernd et al., 2014) to the trenches (Linley et al., 2017) and from the benthic to the pelagic (e.g. Heagney et al., 2007), and has been shown to correlate well with true abundances in experiments (Schobernd et al., 2014; Stoner et al. 2008a). The main criticism of MaxN is that it tends to underestimate true abundances, especially at higher levels of true abundance (Conn, 2011; Schobernd et al., 2014). This makes its use here both conservative and appropriate for comparison to other studies estimating fish abundances.

Even more difficult is extrapolating an absolute density from baited-camera experiments. The arrival rate method (Farnsworth et al., 2007) yields very large estimated absolute densities (18266–28687 fish km^{-2}, Fig. 3c). However, neither the estimated absolute densities calculated using the TOFA method (506–6953 fish km^{-2}, Priede and Merrett 1996) nor the ROV observations (2669 fish km^{-2}) indicate extraordinary densities in our study. There are two possible explanations for this discrepancy. Either the TOFA and ROV estimates are low, or the arrival method gives estimates that are too high, skewed by high MaxN values due to accumulation of fish either through longer individual staying times or greater attraction distances due to higher current velocities on seamounts. While further research is required to differentiate these alternatives, we believe the first is true in this instance for the following reasons.

Several studies have either failed to find a good relationship between 'true' trawl abundance and time of first arrival (eg. Yeh and Drazen 2011) or have shown that MaxN is a more reliable metric (Cappo et al., 2006b; Stoner et al. 2008a). Indeed, in the quickly mounting body of shallow water baited work (BRUVs), MaxN is the standard relative abundance metric used for comparisons and evaluation of abundance (Schobernd et al., 2014). The T_{arr} method was also derived for a specific abyssal species, the rattail *C. armatus* and relies on distribution and behavioral patterns typical of this species (Priede et al., 1990; Priede and Merrett, 1996). Thus, it may not be appropriate for synaphobranchids, for which this method has not been validated. In addition, the T_{arr} model is highly sensitive to low times of first arrival (Farnsworth et al., 2007; Leitner et al., 2017; Linley et al., 2017). T_{arr} values of 1 and 2 min estimate hundreds of thousands and tens of thousands of fish km^{-2}, respectively, which is almost certainly not indicative of true fish abundance, given average estimates of abyssal fish densities across all methods in the 100s of individuals per square kilometer (Fig. 3c, mean= 777 fish km^{-2}). In these 'lucky' drops, the camera likely landed within meters of a fish, and thus such short arrival times are not necessarily related to abundance. Moreover, if video is not continuously recorded, as in this study, the uncertainty of T_{arr} together with this sensitivity makes the use of T_{arr} -estimated densities unreliable and inappropriate in this case. Additionally, disturbance reactions to ROVs are well documented for multiple fish taxa including for the family Synaphobranchidae and have been attributed to the light, noise, water pressure (i.e. bow waves), and electrical fields from ROVs (Ayma et al., 2016; Lorance and Trenkel, 2006; Stoner et al., 2008; Trenkel et al., 2004; Uiblein et al., 2003, 2002). In addition, in our case, ROV surveys available from the seamount were extremely limited in duration, making undercounting of *I. arx* in the seamount ROV surveys more likely.

Finally, we argue against the idea that the high MaxN's are reflective of increased staying time rather than a high local density. Based on optimal foraging theory, it has been suggested (Priede et al., 1990) that staying time will increase in food scarce regions because the probability of finding another meal is low (Charnov, 1976) and thus fish tend to accumulate at bait resulting in a higher MaxN than would be predicted based on local density alone. In the deep sea, food availability is generally thought to correlate well with surface primary productivity and POC flux (Smith et al., 2008). Thus, in a higher productivity deep-sea habitat, fish would be expected to have shorter staying times (the time until MaxN), faster arrival rates, and lower MaxNs (because individuals do not accumulate due to the short staying times) (Priede et al., 1990). With observations from three seamounts that stretch across a productivity gradient, we are able to test this idea and clarify what our high MaxNs really mean. While the mean staying time on the highest productivity seamount was shortest (340 min) as predicted by the optimal foraging-based idea, the arrival rate was actually higher (5 times faster than on the middle productivity seamount), not lower. Moreover, MaxNs were highest at the highest productivity seamount and decreased with decreasing surface productivity/food availability (Suppl. Table 2). Taken together, these observations suggest that the high MaxNs we report here are not reflective of longer staying times, but that the high MaxNs are reflective of high absolute abundance, and that this may be related to food availability. This is also supported in the literature. For example, the previous record abyssal MaxN (68) was recorded in the Arabian Sea under a high productivity regime (Witte, 1999). Likewise, the only other reports of hundreds of fishes at bait parcels come from highly productive regions: the California Margin which experiences coastal upwelling (Smith, 1985; Smith et al., 2002) and the highly productive region around the Falkland Islands (Collins et al., 1999).

The abundance of eels we report here is much higher than any previous report from abyssal depths, and estimated densities are high relative to other studies (Fig. 3). Assuming MaxN is reflective of true abundance, the APEI7 seamount summit could have a higher abundance of fishes than anywhere in the abyssal ocean sampled thus far. Using the best available method for estimating absolute densities, our data suggests densities between 18266 and 28687 fish km^{-2} on the seamount in question here (Fig. 3c). This is at least an order of magnitude higher than the upper estimates for average abyssal fish densities (777 fish km^{-2}) from both trawl and visual transect surveys. At abyssal depths, the highest recorded relative abundance prior to this study comes from a large food fall experiment in the Arabian Sea conducted by Witte, 1999), where after 2 days and 9 h a peak number of 68 zoarcid fishes had gathered around a large, 29 kg shark carcass placed out onto the abyssal plain at 4400 m. Zoarcids are generally necrophagivores rather than active scavengers (necrophages), feeding on the small amphipods that are attracted to carrion in large numbers rather than on the bait itself, though scavenging behavior has been observed occasionally (Jamieson et al., 2017; Jones et al., 1998; Leitner et al., 2017; Witte, 1999). Zoarcids tend to accumulate steadily over time and take up long-term residence around carcasses, making their patterns of arrival at bait distinct from other active scavengers such as the eels observed in our deployments (Jamieson et al., 2017; Jones et al., 1998; Witte, 1999). In fact, the only other reports of large numbers of deep-sea synaphobranchid eels come from two studies at bathyal depths. Jamieson et al. (2017) reported an aggregation with a MaxN of 25 *Synaphobranchus kaupii* from 1419 m off of West Africa, and a second study from the Porcupine Seabight recorded a MaxN of up to 50 *S. kaupii* between 775 and 2467 m at a baited camera system with a maximum estimate of 11, 400 fish km^{-2} from their 1200 m trawl survey (Bailey et al., 2005). Thus, the number of eels observed in this study at abyssal depths is truly unprecedented for both abyssal and bathyal depths.

The high abundances of eels observed may be the result of a 'seamount effect' (Pitcher et al., 2007) in the abyssal ocean. Seamounts are often thought of as biological hotspots supported by locally enhanced productivity (e.g. Clark et al., 2010; Leitner et al., 2020;

Pitcher et al., 2007; Rowden et al., 2010), though few studies (two to date) have ever been conducted on abyssal seamounts. Thus, whether this paradigm can be extended to the deepest and most common seamounts remains uncertain (Wessel et al., 2010). One previous study on an abyssal seamount noted that megafaunal densities were higher on the summit than at equivalent depths on the continental slope (Kaufmann et al., 1989). A second, recent ROV-based study of three abyssal seamounts found a distinct and diverse seamount community characterized by higher abundances of some taxa like asteroids, crinoids, and echinoids, though this study did not include fish (Cuvelier et al., 2020). Studies conducted on abyssal hills, similar but smal'ler features less than 1000 m in height, have reported increased food availability both estimated from overall detritus supply (Durden et al., 2017) and deposited detritus (Morris et al., 2016). In addition abyssal hill studies have found increased megafaunal (Durden et al., 2015, 2020bib_Durden_et_al_2015bib_Durden_et_al_2020) and scavenger abundances (Leitner et al., 2017). However, it should be noted that one study (using un-baited techniques) found no differences in overall fish abundances on an abyssal hill versus on abyssal plains (Milligan et al., 2016). However, at least some evidence exists that abyssal seamounts could host higher abundances of fishes, and our observations of eel aggregations may reflect a general seamount effect. However, clearly not all abyssal seamounts host large populations of fishes because we observed substantially lower numbers of eels on the more northern seamounts. Thus, the southernmost abyssal seamount in APEI 7 may be a particular hotspot, where both a high regional productivity and a local seamount effect may be acting together to create a remarkable abyssal fish hotspot. To test whether this can be generalized broadly to high-productivity abyssal seamounts, a targeted sampling of these features would be required.

It may also be argued that depth (not just food availability) may be decreasing the abundance of these eels across the three seamounts in question because the summit depths get progressively deeper to the northwest, paralleling the decrease in productivity. The observation reported here at 4218 m (DC11 in APEI 1) sets a new depth record for this species. However, from our literature review of abyssal depths, scavenger abundance in general (at least in terms of MaxN) does not seem to be strongly inversely related to depth (Fig. 3b), suggesting that food availability and other environmental and ecological factors may be more important than absolute depth. For example, these eels may be outcompeted on the abyssal plain by specialists like cusk eels and grenadiers, and thus be restricted to the seamount habitat.

It is also possible that the seamount aggregation we observed was a temporary spawning aggregation. Several shallow seamounts (<200 m summit depths) have been shown to be important for eel spawning (Tsukamoto et al., 2003), including eels in family Synaphobranchidae (Fujikura, 1998; Tsukamoto et al., 2003). However, none of the 12 captured specimens were gravid females (in fact most were juveniles), which speaks against the spawning aggregation hypothesis in this case and suggests that this aggregation may not be a temporary phenomenon.

Given that *I. arx* was exclusively observed on seamount habitats, it seems possible that this species may be a seamount specialist; however, little information exists on this species. The only other in-situ observations of *I. arx* stem from other seamounts and come from the NOAA Campaign to Address Pacific monument Science, Technology, and Ocean NEeds (CAPSTONE) project, which observed *Ilyophis arx* during ROV surveys of seamounts and island flanks in the western Pacific Ocean (NOAA, 2020). In addition, all *I. arx* specimens in collections worldwide (N=6) have also been collected from seamounts, ridges, and islands in the Pacific. Thus, while limited, all information to date suggest an association of *Ilyophis arx* with abrupt topographies.

5. Conclusions and future directions

We report the highest number of fishes ever recorded at carrion at abyssal depths and the first ever observations of large aggregations of eels at these depths. Traditionally, the abyssal seafloor is considered a habitat of low megafaunal abundances with populations limited by challenging environmental conditions (low food availability, low temperatures, high pressures), but these generalizations may not apply to seamount summits at abyssal depths. How can such high numbers of active megafaunal predators be sustained in a relatively small and seemingly isolated area of the abyssal seafloor on a seamount summit? Are these eels permanent seamount residents or were these ephemeral aggregations? Abyssal seamounts may provide unusual laboratories in which to explore carbon flows and energy availability in abyssal food webs with a high abundance of top predators.

CRediT authorship contribution statement

Astrid B. Leitner: Conceptualization, Methodology, Formal analysis, Investigation, Writing - original draft, Funding acquisition. **Jennifer M. Durden:** Data curation, Writing - review & editing, Project administration. **Craig R. Smith:** Conceptualization, Investigation, Resources, Writing - review & editing, Supervision, Project administration, Funding acquisition. **Eric D. Klingberg:** Investigation, Writing - review & editing. **Jeffrey C. Drazen:** Conceptualization, Methodology, Investigation, Resources, Writing - original draft, Writing - review & editing, Supervision, Project administration, Funding acquisition.

Declaration of competing interest

The authors declare that they have no known competing financial interests or personal relationships that could have appeared to influence the work reported in this paper.

Acknowledgments

We acknowledge the captain and crew of the RV *Kilo Moana*, the team of the remotely-operated vehicle *Lu'ukai,* and the science team of the DeepCCZ expedition for making this research possible. We thank taxonomic experts David G. Smith and Kenneth Tighe of the Smithsonian Institute for assistance with identification of all trapped specimens, and Ben Frable and Philip A. Hastings of the Scripps Institute of Oceanography fish collection for allowing us to examine the synaphobranchid specimens archived there. We thank Kirsty McQuaid and Kerry Howell for extracting the seafloor POC flux for our deployment locations from the Lutz et al., (2007) model. We also thank the NOAA Office of Ocean Exploration (grant # NA17OAR0110209) and the Gordon and Betty Moore Foundation (grant no. 5596) for financial support. We also would like to thank the School of Ocean and Earth, Science and Technology at the University of Hawaii, which funded 3 of the seamount ROV dives conducted by its 6000 m rated ROV *Lu'ukai*. This is SOEST contribution #XXXX.

Appendix A. Supplementary data

Supplementary data to this article can be found online at https://doi.org/10.1016/j.dsr.2020.103423.

References

Auster, P.J., Cantwell, K., Grubbs, R.D., Hoy, S., 2020. Observations of deep-sea sharks and associated species at a large food fall on the continental margin off South Carolina , USA (NW Atlantic). J. Ocean Sci. Found. 35, 48–53. https://doi.org/10.5281/zenodo.3932138.

Ayma, A., Aguzzi, J., Canals, M., Lastras, G., Bahamon, N., Mecho, A., Company, J.B., 2016. Comparison between ROV video and Agassiz trawl methods for sampling deep water fauna of submarine canyons in the Northwestern Mediterranean Sea with observations on behavioural reactions of target species. Deep. Res. Part I Oceanogr. Res. Pap. 114, 149–159. https://doi.org/10.1016/j.dsr.2016.05.013.

Bailey, D.M., Genard, B., Collins, M. a, Rees, J.-F., Unsworth, S.K., Battle, E.J.V., Bagley, P.M., Jamieson, A.J., Priede, I.G., 2005. High swimming and metabolic activity in the deep-sea eel Synaphobranchus kaupii revealed by integrated in situ and in vitro measurements. Physiol. Biochem. Zool. 78, 335–346. https://doi.org/10.1086/430042.

Bailey, D.M., Ruhl, H.A., Smith, K.L., 2006. Long-term change in benthopelagic fish abundance in the abyssal northeast Pacific Ocean. Ecology 87, 549–555.
Becker, J.J., Sandwell, D.T., Smith, W.H.F., Braud, J., Binder, B., Depner, J., Fabre, D., Factor, J., Ingalls, S., Kim, S.-H., Ladner, R., Marks, K., Nelson, S., Pharaoh, a., Trimmer, R., Von Rosenberg, J., Wallace, G., Weatherall, P., 2009. Global bathymetry and elevation data at 30 arc seconds resolution: SRTM30_PLUS. Mar. Geodes. 32, 355–371. https://doi.org/10.1080/01490410903297766.
Cailliet, G.M., Andrews, A.H., Wakefield, W.W., Moreno, G., Rhodes, K.L., 1999. Fish faunal and habitat analyses using trawls, camera sleds and submersibles in benthic deep-sea habitats off central California. Oceanol. Acta 22, 579–592. https://doi.org/10.1016/S0399-1784(00)88949-5.
Cappo, M., Harvey, E., Shortis, M., 2006a. Counting and measuring fish with baited video techniques - an overview. Cutting-Edge Technol. Fish Fish. Sci. 101–114 https://doi.org/10.1007/978-1-62703-724-2_1.
Cappo, M., Harvey, E.S., Shortis, M., 2006b. Counting and measuring fish with baited video techniques – an overview. Australian Society for Fish Biology Workshop Proceedings, pp. 101–114. https://doi.org/10.1007/978-1-62703-724-2_1.
Charnov, E.L., 1976. Optimal foraging, the marginal value theorem. Theor. Popul. Biol. 9, 129–136. https://doi.org/10.1016/0040-5809(76)90040-X.
Clark, M.R., Rowden, A.A., Schlacher, T., Williams, A., Consalvey, M., Stocks, K.I., Rogers, A.D., O'Hara, T.D., White, M., Shank, T.M., Hall-Spencer, J.M., 2010. The ecology of seamounts: structure, function, and human impacts. Ann. Rev. Mar. Sci. 2, 253–278. https://doi.org/10.1146/annurev-marine-120308-081109.
Collins, M.A., Priede, I.G., Bagley, P.M., 1999a. In situ comparison of activity in two deep-sea scavenging fishes occupying different depth zones. Proc. R. Soc. B Biol. Sci. 266, 2011. https://doi.org/10.1098/rspb.1999.0879.
Collins, M.A., Yau, C., Nolan, C.P., Bagley, P.M., Priede, I.G., 1999b. Behavioural observations on the scavenging fauna of the Patagonian slope. J. Mar. Biol. Assoc. U. K. 79, 963–970. https://doi.org/10.1017/S0025315499001198.
Conn, P.B., 2011. An Evaluation and Power Analysis of Fishery Independent Reef Fish Sampling in the Gulf of Mexico and U.S. South Atlantic.
Cousins, N.J., Shields, M.A., Crockard, D., Priede, I.G., 2013a. Bathyal demersal fishes of charlie gibbs fracture zone region (49-54°N) of the mid-atlantic ridge, I: results from trawl surveys. Deep. Res. Part II Top. Stud. Oceanogr. 98, 388–396. https://doi.org/10.1016/j.dsr2.2013.08.012.
Cousins, N.J., Shields, M.A., Crockard, D., Priede, I.G., 2013b. Bathyal demersal fishes of charlie gibbs fracture zone region (49-54°N) of the mid-atlantic ridge, I: results from trawl surveys. Deep. Res. Part II Top. Stud. Oceanogr. 98, 388–396. https://doi.org/10.1016/j.dsr2.2013.08.012.
Cuvelier, D., Ribeiro, P., Ramalho, S., Kersken, D., Martinez Arbizu, P., Colaço, A., 2020. Are seamounts refuge areas for fauna from polymetallic nodule fields? Biogeosci. Discuss. 2657–2680. https://doi.org/10.5194/bg-2019-304.
Drazen, J.C., Church, M., Dahlgren, T.G., Durden, J.M., Glover, A.G., Goetze, E., Leitner, A.B., Smith, C.R., Sweetman, A.K., 2019. Exploration of biodiversity and ecosystem structure on seamounts in the western CCZ. New Front. Ocean Explor. E/V Naut. NOAA Sh. Okeanos Explor. R/V Falkor 2018 F. Seas. 32, 120.
Drazen, J.C., Popp, B.N., Choy, C.A., Clemente, T., De Forest, L., Smith Jr., K.L., Smith, K. L.J., 2008. Bypassing the abyssal benthic food web: macrourid diet in the eastern North Pacific inferred from stomach content and stable isotopes analyses. Limnol. Oceanogr. 53, 2644. https://doi.org/10.4319/lo.2008.53.6.2644.
Drazen, J.C., Sutton, T.T., 2017. Dining in the Deep : the feeding ecology of deep-sea fishes. Ann. Rev. Mar. Sci. 9, 1–26. https://doi.org/10.1146/annurev-marine-010816-060543.
Durden, J.M., Bett, B.J., Jones, D.O.B., Huvenne, V.a.I., Ruhl, H.a., 2015. Abyssal hills – hidden source of increased habitat heterogeneity, benthic megafaunal biomass and diversity in the deep sea. Prog. Oceanogr. 137, 209–218. https://doi.org/10.1016/j.pocean.2015.06.006.
Durden, J.M., Bett, B.J., Ruhl, H.A., 2020. Subtle variation in abyssal terrain induces significant change in benthic megafaunal abundance, diversity, and community structure. Prog. Oceanogr. 186, 102395. https://doi.org/10.1016/j.pocean.2020.102395.
Durden, J.M., Ruhl, H.A., Pebody, C., Blackbird, S.J., van Oevelen, D., 2017. Differences in the carbon flows in the benthic food webs of abyssal hill and plain habitats. Limnol. Oceanogr. 62, 1771–1782. https://doi.org/10.1002/lno.10532.
Farnsworth, K.D.D., Thygesen, U.H.H., Ditlevsen, S., King, N.J.J., 2007. How to estimate scavenger fish abundance using baited camera data. Mar. Ecol. Prog. Ser. 350, 223–234. https://doi.org/10.3354/meps07190.
Fleury, A.G., Drazen, J.C., 2013. Abyssal scavenging communities attracted to sargassum and fish in the sargasso sea. Deep. Res. Part I Oceanogr. Res. Pap. 72, 141–147. https://doi.org/10.1016/j.dsr.2012.11.004.
Fujikura, K., 1998. Investigation of the deep-sea chemosynthetic ecosystem and submarine volcano at the kaguga 2 and 3 seamounts in the northern mariana trough, western pacific. Deep Sea Res. 127–138.
Hardinge, Jethro, Harvey, Euan S., Saunders, Benjamin J., Newman, Stephen J., 2013. A little bait goes a long way: The influence of bait quantity on a temperate fish assemblage sampled using stereo-BRUVs. J. Exp. Mar. Biol. Ecol. 449, 250–260. https://doi.org/10.1016/j.jembe.2013.09.018.
Harris, P.T., Macmillan-Lawler, M., Rupp, J., Baker, E.K., 2014. Geomorphology of the oceans. Mar. Geol. 352, 4–24. https://doi.org/10.1016/j.margeo.2014.01.011.
Heagney, E., Lynch, T., Babcock, R., Suthers, I., 2007. Pelagic fish assemblages assessed using mid-water baited video: standardising fish counts using bait plume size. Mar. Ecol. Prog. Ser. 350, 255–266. https://doi.org/10.3354/meps07193.
Jamieson, A.J., Linley, T.D., Craig, J., 2017. Baited camera survey of deep-sea demersal fishes of the West African oil provinces off Angola: 1200–2500m depth, East Atlantic Ocean. Mar. Environ. Res. 129, 347–364. https://doi.org/10.1016/j.marenvres.2017.05.009.
Jones, E.G., Collins, M.A., Bagley, P.M., Addison, S., Priede, I.G., 1998. The fate of cetacean carcasses in the deep sea: observations on consumption rates and succession of scavenging species in the abyssal north-east Atlantic Ocean. Proc. R. Soc. B Biol. Sci. 265, 1119–1127. https://doi.org/10.1098/rspb.1998.0407.
Kaufmann, R.S., Wakefield, W.W., Genin, A., 1989. Distribution of epibenthic megafauna and lebensspuren on two central north Pacific seamounts. Deep Sea Res. 36, 1863.
Lauth, R.R., Ianelli, J., Wakefield, W.W., 2004. Estimating the size selectivity and catching efficiency of a survey bottom trawl for thornyheads, Sebastolobus spp. using a towed video camera sled. Fish. Res. 70, 27–37. https://doi.org/10.1016/j.fishres.2004.06.010.
Leitner, A.B., Neuheimer, A.B., Donlon, E., Smith, C.R., Drazen, J.C., 2017. Environmental and bathymetric influences on abyssal bait-attending communities of the Clarion Clipperton Zone. Deep. Res. Part I Oceanogr. Res. Pap. 125, 65–80. https://doi.org/10.1016/j.dsr.2017.04.017.
Leitner, A.B., Neuheimer, A.B., Drazen, J.C., 2020. Evidence for long-term seamount-induced chlorophyll enhancements. Sci. Rep. 10, 1–10. https://doi.org/10.1038/s41598-020-69564-0.
eitner, Astrid B., Smith, Craig R., Drazen, Jeffrey C., n.d.. Testing the seamount refuge hypothesis for predators and scavengers in the western Clarion-Clipperton Zone. Frontiers of Marine Science. In preparation.
Linley, Thomas D., Stewart, A.L., McMillan, P.J., Clark, Malcolm R., Gerringer, Mackenzie E., Drazen, Jeffrey C., Fujii, Toyonobu, Jamieson, Alan J., 2017. Bait attending fishes of the abyssal zone and hadal boundary: community structure, functional groups and species distribution in the Kermadec, New Hebrides and Mariana trenches. Deep-Sea Res. Part I Oceanogr. Res. Pap. 121, 38–53. https://doi.org/10.1016/j.dsr.2016.12.009.
Lorance, P., Trenkel, V.M., 2006. Variability in natural behaviour, and observed reactions to an ROV, by mid-slope fish species. J. Exp. Mar. Biol. Ecol. 332, 106–119. https://doi.org/10.1016/j.jembe.2005.11.007.
Lutz, M.J., Caldeira, K., Dunbar, R.B., Behrenfeld, M.J., 2007. Seasonal rhythms of net primary production and particulate organic carbon flux to depth describe the efficiency of biological pump in the global ocean. J. Geophys. Res. 112, C10011. https://doi.org/10.1029/2006JC003706.
Merrett, N.R., Gordon, J.D.M., Stehmann, M., Haedrich, R.L., 1991. Deep demersal fish assemblage structure in the porcupine seabight (Eastern north atlantic): slope sampling by three different trawls compared. J. Mar. Biol. Assoc. U. K. 71, 329–358. https://doi.org/10.1017/S0025315400051638.
Milligan, R.J., Morris, K.J., Bett, B.J., Durden, J.M., Jones, D.O.B., Robert, K., Ruhl, H.A., Bailey, D.M., 2016. High resolution study of the spatial distributions of abyssal fishes by autonomous underwater vehicle. Sci. Rep. 6, 1–12. https://doi.org/10.1038/srep26095.
Misa, W.F.X.E., Richards, B.L., DiNardo, G.T., Kelley, C.D., Moriwake, V.N., Drazen, J.C., 2016. Evaluating the effect of soak time on bottomfish abundance and length data from stereo-video surveys. J. Exp. Mar. Biol. Ecol. 479, 20–34. https://doi.org/10.1016/j.jembe.2016.03.001.
Morris, K.J., Bett, B.J., Durden, J.M., Benoist, N.M.A., Huvenne, V.A.I., Jones, D.O.B., Robert, K., Ichino, M.C., Wolff, G.A., Ruhl, H.A., 2016. Landscape-scale spatial heterogeneity in phytodetrital cover and megafauna biomass in the abyss links to modest topographic variation. Sci. Rep. 6, 34080. https://doi.org/10.1038/srep34080.
National Oceanic & Atmospheric Administration NOAA, 2020. deep-sea fishes observed during NOAA's Office of Ocean exploration and research CAPSTONE ROV surveys in the central and western pacific (2015-2017). In: Records provided by the Hawai'i Undersea Research Laboratory, University of Hawai'i, to NOAA's Deep Sea Coral Research & Technology Program..
Pearcy, W.G., Stein, D.L., Carney, R.S., 1982. The deep-sea benthic fish fauna of the northeastern Pacific Ocean on Cascadia and Tufts abyssal plains and adjoining continental slopes. Biol. Oceanogr. 1, 375–428.
Seamounts: Ecology, Fisheries and Conservation. Blackwell Fisheries and Aquatic Resources Series. In: Pitcher, T.J., Morato, T., Hart, P.J.B., Clark, M.R., Haggan, N., Santos, R.S. (Eds.), 2007, vol. 12. Blackwell Publishing, Oxford.
Priede, I., 2017. Deep-sea Fishes: Biology, Diversity, Ecology and Fisheries. Cambridge University Press.
Priede, I.G., Merrett, N.R., 1996. Estimation of abundance of abyssal demersal fishes; a comparison of data from trawls and baited cameras. J. Fish. Biol. 49, 207–216. https://doi.org/10.1111/j.1095-8649.1996.tb06077.x.
Priede, I.G., Smith, K.L., Armstrong, J.D., 1990. Foraging behavior of abyssal grenadier fish: inferences from acoustic tagging and tracking in the North Pacific Ocean. Deep Sea Res. Part A. Oceanogr. Res. Pap. 37, 81–101. https://doi.org/10.1016/0198-0149(90)90030-Y.
Rowden, A.A., Dower, J.F., Schlacher, T.A., Consalvey, M., Clark, M.R., 2010. Paradigms in seamount ecology: fact, fiction and future. Mar. Ecol. 31, 226–241. https://doi.org/10.1111/j.1439-0485.2010.00400.x.
Sackett, D.K., Kelley, C.D., Drazen, J.C., 2017. Spilling over deepwater boundaries : evidence of spillover from two deepwater restricted fishing areas in Hawaii. Mar. Ecol. Prog. Ser. 568, 175–190.
Sainte-Marie, B., Hargrave, B.T., 1987. Estimation of scavenger abundance and distance of attraction to bait. Mar. Biol. 94, 431–443.
Schobernd, Z.H., Bacheler, N.M., Conn, P.B., 2014. Examining the utility of alternative video monitoring metrics for indexing reef fish abundance. Can. J. Fish. Aquat. Sci. 71, 464–471. https://doi.org/10.1139/cjfas-2013-0086.
Smith, C.R., 1985. Food for the deep sea: utilization, dispersal, and flux of nekton falls at the Santa Catalina Basin floor. Deep Sea Res. 32, 417–442.
Smith, C.R., Baco, A.R., Glover, A.G., 2002. Faunal succession on replicate deep-sea whale falls: time scales and vent-seep affinities. Cah. Biol. Mar. 43, 293–297.

Smith, C.R., Berelson, W., Demaster, D.J., Dobbs, F.C., Hammond, D., Hoover, D.J., Pope, R.H., Stephens, M., 1997. Latitudinal variations in benthic processes in the abyssal equatorial Pacific: control by biogenic particle flux. Deep. Res. Part II Top. Stud. Oceanogr. 44, 2295–2317. https://doi.org/10.1016/S0967-0645(97)00022-2.

Smith, C.R., De Leo, F.C., Bernardino, A.F., Sweetman, A.K., Arbizu, P.M., 2008. Abyssal food limitation, ecosystem structure and climate change. Trends Ecol. Evol. 23, 518–528.

Smith, C.R., Demopoulos, A.W., 2003. The deep Pacific ocean floor. In: Ecosystems of the Deep Oceans, vol. 28, pp. 179–218.

Stoner, A.W., Laurel, B.J., Hurst, T.P., 2008. Using a baited camera to assess relative abundance of juvenile Pacific cod: field and laboratory trials. J. Exp. Mar. Biol. Ecol. 354, 202–211. https://doi.org/10.1016/j.jembe.2007.11.008.

Stoner, Allan W., Ryer, C.H., Parker, S.J., Auster, P.J., Wakefield, W.W., 2008b. Evaluating the role of fish behavior in surveys conducted with underwater vehicles. Can. J. Fish. Aquat. Sci. 65, 1230–1243. https://doi.org/10.1139/F08-032.

Trenkel, V.M., Lorance, P., Mahévas, S., 2004. Do visual transects provide true population density estimates for deepwater fish? ICES J. Mar. Sci. J. du Cons. 61, 1050–1056.

Tsukamoto, K., Otake, T., Mochioka, N., Lee, T.-W., Fricke, H., Inagaki, T., 2003. Seamounts new moon and eel spawning. Environ. Biol. Fish. 66, 221–229.

Uiblein, F., Lorance, P., Latrouite, D., 2003. Behaviour and habitat utilisation of seven demersal fish species on the Bay of Biscay continental slope, NE Atlantic. Mar. Ecol. Prog. Ser. 257, 223–232. https://doi.org/10.3354/meps257223.

Uiblein, F., Lorance, P., Latrouite, D., 2002. Variation in locomotion behaviour in northern cutthroat eel (Synaphobranchus kaupi) on the Bay of Biscay continental slope. Deep. Res. Part I Oceanogr. Res. Pap. 49, 1689–1703. https://doi.org/10.1016/S0967-0637(02)00065-1.

Wedding, L.M., Friedlander, A.M., Kittinger, J.N., Watling, L., Gaines, S.D., Bennett, M., Hardy, S.M., Smith, C.R., 2013. From principles to practice: a spatial approach to systematic conservation planning in the deep sea. Proc. Biol. Sci. 280, 20131684. https://doi.org/10.1098/rspb.2013.1684.

Wessel, P., Sandwell, D.T., Kim, S.-S., 2010. The global seamount census. Oceanography 23, 24.

Witte, U., 1999. Consumption of large carcasses by scavenger assemblages in the deep Arabian Sea: observations by baited camera. Mar. Ecol. Prog. Ser. 183, 139–147. https://doi.org/10.3354/meps183139.

Yeh, J., Drazen, J.C., 2011. Baited-camera observations of deep-sea megafaunal scavenger ecology on the California slope. Mar. Ecol. Prog. Ser. 424, 145–156. https://doi.org/10.3354/meps08972.

Yeh, J., Drazen, J.C., 2009. Depth zonation and bathymetric trends of deep-sea megafaunal scavengers of the Hawaiian Islands. Deep. Res. Part I Oceanogr. Res. Pap. 56, 251–266. https://doi.org/10.1016/j.dsr.2008.08.005.